IOP Conf. Series: Materials Science and Engineering **63** (2014) 012046 doi:10.1088/1757-899X/63/1/012046

Effect of geometric parameters on deformation behavior of simple shear extrusion

E Bagherpour[1], F Qods[2], R Ebrahimi[3]

[1]Ph.D. student, Faculty of Metallurgical and Materials Engineering, Semnan University, Semnan, Iran
Email: ebad.bagherpoor@gmail.com

[2] Associate Professor, Faculty of Metallurgical and Materials Engineering, Semnan University, Semnan, Iran
Email: qods@semnan.ac.ir

[3] Associate Professor, Department of Materials Science and Engineering, School of Engineering, Shiraz University, Shiraz, Iran
Email: ebrahimy@shirazu.ac.ir

Abstract. In the present study, the effect of geometric parameters on the simple shear extrusion (SSE) process as one of the most recent severe plastic deformation methods is investigated. Three deferent curvatures for deformation channel based on linear, quadratic and sine equations are introduced. Simulation of the process is carried out by means of the commercial finite element code ABAQUS/Explicit. Effect of die profile as well as backpressure on the strain, strain rate and load of deformation is studied. Results show that the shape of die profile does not have any significant effect on the required backpressure and the load of the process. The most homogeneous distribution of strain is obtained by linear die profile. Among all die profiles, only the linear profile can provide a constant strain rate. It is shown that linear profile is also the best candidate for deformation channel in SSE process due to its feasibility and homogeneity in the distribution of stain and constant strain rate.

Keywords: severe plastic deformation, simple shear extrusion, finite element analysis, geometric parameters, die profile.

1. Introduction

In recent years, ultra-fine grained (UFG) materials have been widely studied due to their excellent mechanical and physical properties, such as high strength and ductility [1, 2]. Nowadays, severe plastic deformation (SPD) is considered as a promising method for producing bulk nano-structured materials [3]. The basic and most familiar SPD techniques include equal channel angular pressing (ECAP)[4], high-pressure torsion[5], accumulative roll bonding[6], multi-directional forging(MDF)[7] and twist extrusion (TE)[8]. The increasing interest of materials scholars to produce bulk nanostructured materials has led to development of new SPD methods such as constraint groove pressing(CGP)[9], simple shear extrusion (SSE)[10], cyclic expansion–extrusion (CEE)[11], vortex extrusion (VE)[12] and so on. Among all these methods, TE and SSE are based on direct extrusion and they can be easily installed on any standard extrusion equipment or set in industrial production lines [10, 13]. From the time of introduction to now, many researches were conducted to clarify different aspect of TE technique [1, 8, 13,

14].On the other hands only a slight attempt has been made to investigate different aspects of SSE method and they are still unknown.

SSE technique was introduced in 2009 by Pardis and Ebrahimi[10] based on pressing material through a specially designed direct extrusion channel. Using finite element analysis and experiments on commercially pure aluminum (AA1050), they concluded that this method was capable of imposing strain to the materials without any significant change in specimen's shape and geometry. They also revealed that SSE is more beneficial because the amount of waste material is negligible compared with that of ECAP. They concluded that the distribution of strain is more symmetrical (homogeneous) through cross section of the sample, which is a great advantage of this method compared to other SPD techniques. In 2010, Pardis and Ebrahimi[15] introduced four different processing routes (A–D) for deformation via simple shear extrusion process. They reported that the variation of shear strain was the same in routes B and C while the homogeneity was improved in route C due to 90° rotation of the sample about its main axis. Bagherpour et al. [16] processed a twinning induced plasticity (TWIP) steel by ECAP and SSE processes. They showed that single pass of ECAP leads to the segmented flow as a result of flow localization while SSE could deform the TWIP steel without observation of any segmentation due to its quite larger deformation zone compared with that of ECAP. In other words, the strain in SSE is imposed gradually while in ECAP, it is inserted in a localized region. Bagherpour et al.[17] in other publication, investigated the microstructure and deformation behavior of TWIP steel processed by SSE. They showed that the dislocation density increased from start to the middle of the deformation channel and reduced in the second half of the channel due the strain reversal and annihilation of dislocation in the second half of the SSE channel. Bayat Tork et al. [18] investigated the feasibility of room temperature plastic deformation of pure magnesium through SSE. They showed that samples processed by ECAP, channel angular deformation (CAD) and dual equal channel lateral extrusion (DECLE) were severely segmented due to the localized shear strain applied along the shear plane, while the samples processed by SSE exhibited no significant segmentation. They concluded that SSE is the most promising technique for room temperature processing of magnesium with the aim to refine the microstructure.

Until now, the die profile of the SSE has been determined by combination of several quadratic equations. In the present study, sine and linear profiles are introduced and the effect of these profiles on deformation behavior of materials during the process is investigated by finite element method using ABAQUS/Explicit package.

2- Deformation channel profiles

During SSE the sample is pressed through a direct channel with a specific shape (profile). As the specimen passes through the channel, it deforms gradually while its cross-section area remains constant. In this process, samples are chosen with square cross section. As it can be seen in Fig.1, by passing through the extrusion channel, the material undergoes shear deformation by changing the shape of cross-section from a square at the entrance of the channel to a parallelogram with the maximum distortion angle (α_{max}) at the middle of the channel, and back to square at the exit. All the planes in Fig.1 have the same area. By passing the material through the first half of channel, position of point A_o is changed along y-direction in yz plane by the amount of d_x (see Fig.1). As a result of this translation, the material is distorted by the angle of α_x. Therefore, by passing the material through sections $S_{\Delta x}$ and $S_{L/2}$, point A_o shifts gradually to

points $A_{\Delta x}$ and $A_{L/2}$, respectively. Hence, the square cross-section of S_o at the entrance of the channel is changed to the parallelograms of $S_{\Delta x}$ and $S_{L/2}$ and the material is distorted by the angles of $\alpha_{\Delta x}$ and α_{max}, respectively. In the other words, the distortion angle is changed from o to α_{max} through the first half of the deformation channel. Through the second half of deformation channel (from $L/2$ to L through x-direction), the point $A_{L/2}$ gradually shifts to $A_{\Delta x}$ and, finally, at the exit it backs to its original place of A_o (the distortion angle is changed from α_{max} to o). As it can be seen, sections in the x-directions of Δx and L- Δx have the same d_x ($d_{\Delta x}$) and distortion angle ($\alpha_{\Delta x}$).

Changing the position of point A_o to $A_{\Delta x}$ and $A_{L/2}$ and going back to A_o by variation of d_x with x-direction, a curve in xy plane is made which describe the profile of the deformation channel. In the present section, three deferent curvatures for deformation channel based on linear, quadratic and sine equations are introduced.

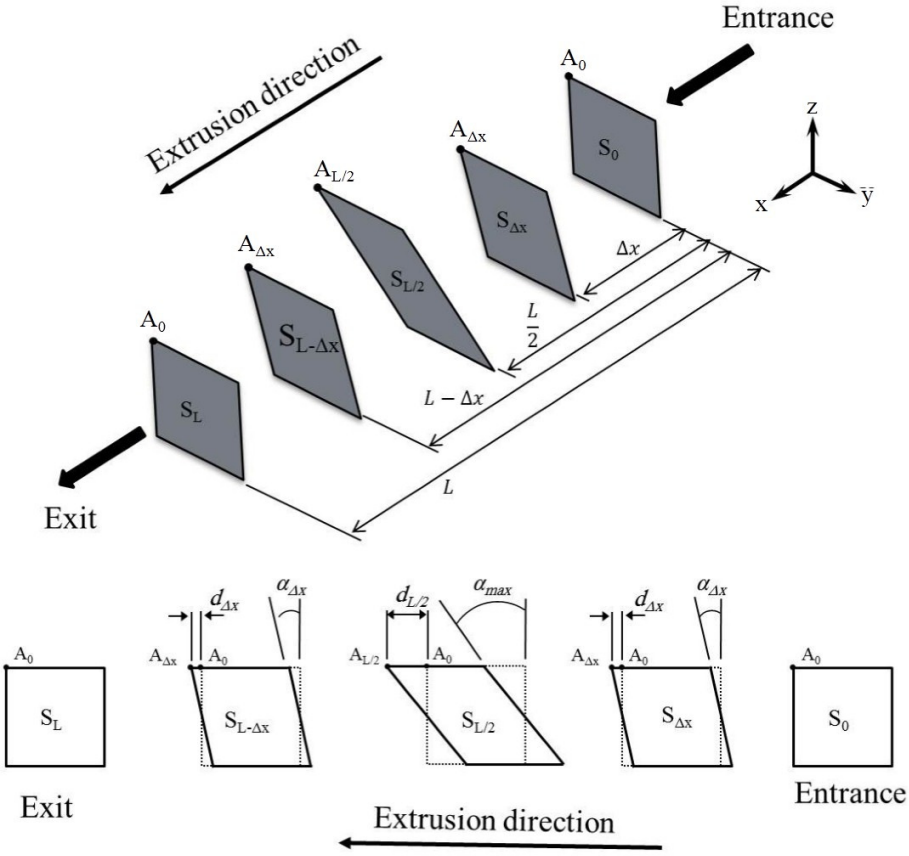

Fig.1. Schematic of sections through deformation channel

As previously mentioned, from the time of invention of SSE to now, only a quadratic profile has been considered for SSE channel. For a quadratic form of the die profile, d_x is calculated by

$$d_x = \begin{cases} \frac{4a\tan\alpha_{\max}}{L^2}x^2 & 0 \le x \le \frac{L}{4} \\ -\frac{4a\tan\alpha_{\max}}{L^2}(x-\frac{L}{2})^2 + \frac{a\tan\alpha_{\max}}{2} & \frac{L}{4} \le x \le \frac{3L}{4} \\ \frac{4a\tan\alpha_{\max}}{L^2}(x-L)^2 & \frac{3L}{4} \le x \le L \end{cases} \quad (1)$$

where a is the side of the square cross section in the entrance of the channel, L is the length of the deformation channel, α_{max} is the maximum distortion angle and x is the distance of each plane from the channel inlet.

For a sinusoidal die profile, d_x is calculated as

$$d_x = \frac{a\tan\alpha_{\max}}{2}\sin(\frac{\pi}{L}x)\,. \quad (2)$$

Linear profile is designed so that the d_x is obtained by

$$d_x = \begin{cases} \frac{a\tan\alpha_{\max}}{L}x & 0 \le x \le \frac{L}{2} \\ -\frac{a\tan\alpha_{\max}}{L}x + a\tan\alpha_{\max} & \frac{L}{2} \le x \le L \end{cases} \quad . \quad (3)$$

Fig.2 shows the quadratic, sinusoidal and linear profiles for a deformation channel with the dimensions 60×10×10 mm. The maximum distortion angle of 45^o [10, 15-18] is considered.

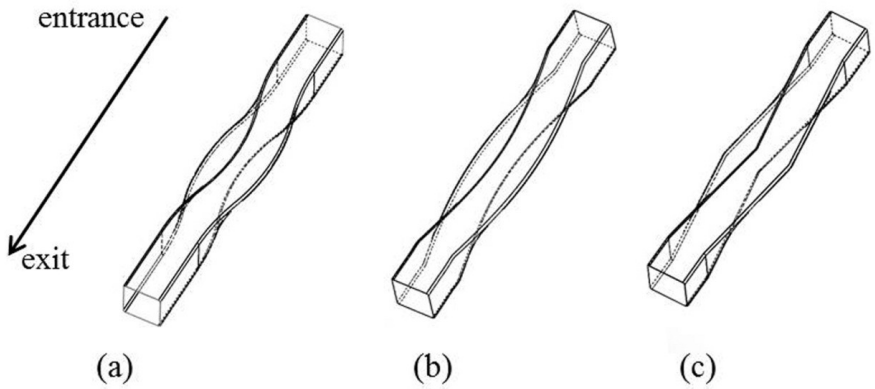

Fig.2. Different SSE profiles, (a) quadratic, (b) sinusoidal and (c) linear.

3- Strain and Strain rate

In order to calculate the strain in this process, the initially square planar section normal to direction of extrusion is studied. This section deforms under shear while passing through the first half of the channel. The same shear strain is accumulated as the element deforms back to its initial configuration, while passing through the second half of the channel[10] (Fig.1). Therefore, for SSE process with the maximum distortion angle of α_{max}, the total shear strain, γ, is given by[10]:

$$\gamma = 2\tan(\alpha_{\max}). \tag{4}$$

According to Mises criterion, the total equivalent strain, ε_{eq}, is calculated by

$$\varepsilon_{eq} = \frac{\gamma}{\sqrt{3}}. \tag{5}$$

Fig.3 shows a plane located at the x distance from the channel inlet (x-plane). It is clear that the plastic shear strain (γ_x) for the selected plane is calculated by

$$\gamma_x = \tan(\alpha) = \frac{d_x}{\frac{a}{2}} = \frac{2d_x}{a}. \tag{6}$$

By inserting Eqs. (1) and (6) into Eq. (5), the equivalent accumulate strain for the quadratic profile is determined as

$$\varepsilon_{eq}^{x} = \begin{cases} \dfrac{8\tan\alpha_{\max}}{L^2\sqrt{3}}x^2 & 0 \le x \le \dfrac{L}{4} \\ -\dfrac{8\tan\alpha_{\max}}{L^2\sqrt{3}}(x-\dfrac{L}{2})^2 + \dfrac{\tan\alpha_{\max}}{\sqrt{3}} & \dfrac{L}{4} \le x \le \dfrac{L}{2} \\ \dfrac{8\tan\alpha_{\max}}{L^2\sqrt{3}}(x-\dfrac{L}{2})^2 + \dfrac{\tan\alpha_{\max}}{\sqrt{3}} & \dfrac{L}{2} \le x \le \dfrac{3L}{4} \\ -\dfrac{8\tan\alpha_{\max}}{L^2\sqrt{3}}(x-L)^2 + \dfrac{2\tan\alpha_{\max}}{\sqrt{3}} & \dfrac{3L}{4} \le x \le L \end{cases}. \tag{7}$$

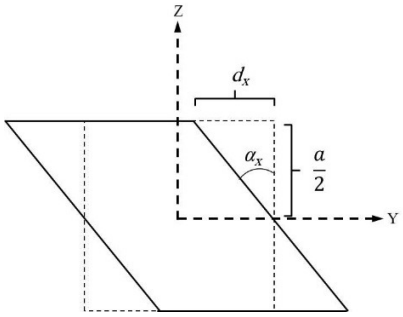

Fig.3. The plane section located at the *x* distance from the channel inlet

It should be mentioned that to calculate the effective strain of the sections located in the second half of the channel, the imposed shear strain of the first half of the channel should be considered. Differentiating Eq. (11) with respect to time (*t*), gives the current strain rate ~~is calculated~~ as

$$\dot{\varepsilon}_x = \begin{cases} \dfrac{16\tan\alpha_{\max}}{L^2\sqrt{3}} x \dfrac{dx}{dt} & 0 \le x \le \dfrac{L}{4} \\ -\dfrac{16\tan\alpha_{\max}}{L^2\sqrt{3}} (x - \dfrac{L}{2}) \dfrac{dx}{dt} & \dfrac{L}{4} \le x \le \dfrac{L}{2} \\ \dfrac{16\tan\alpha_{\max}}{L^2\sqrt{3}} (x - \dfrac{L}{2}) \dfrac{dx}{dt} & \dfrac{L}{2} \le x \le \dfrac{3L}{4} \\ -\dfrac{16\tan\alpha_{\max}}{L^2\sqrt{3}} (x - L) \dfrac{dx}{dt} & \dfrac{3L}{4} \le x \le L \end{cases} \tag{8}$$

where $\dfrac{dx}{dt}$ is the ram speed.

Using the same procedure as quadratic profile the strain and current strain rate of the sinusoidal profile, are determined by

$$\varepsilon_{eq}^{x} = \begin{cases} \dfrac{\tan\alpha_{\max}}{\sqrt{3}} \sin(\dfrac{\pi}{L} x) & 0 \le x \le \dfrac{L}{2} \\ \dfrac{\tan\alpha_{\max}}{\sqrt{3}} (2 - \sin(\dfrac{\pi}{L} x)) & \dfrac{L}{2} \le x \le L \end{cases} \tag{9}$$

and

$$\dot{\varepsilon}_x = \begin{cases} \dfrac{\pi \tan \alpha_{\max}}{L\sqrt{3}} \cos(\dfrac{\pi}{L} x) \dfrac{dx}{dt} & 0 \le x \le \dfrac{L}{2} mm \\ \dfrac{\pi \tan \alpha_{\max}}{L\sqrt{3}} \cos(\dfrac{\pi}{L} x) \dfrac{dx}{dt} & \dfrac{L}{2} \le x \le L mm \end{cases} . \quad (10)$$

For the case of linear die profile, the equivalent strain and the instantaneous strain rate are determined by

$$\varepsilon_{eq}^{x} = \frac{2 \tan \alpha_{\max}}{\sqrt{3}L} x \quad (11)$$

and

$$\dot{\varepsilon}_x = \frac{2 \tan \alpha_{\max}}{\sqrt{3}L} \frac{dx}{dt} . \quad (12)$$

3- Finite element analysis

The commercial finite element code, ABAQUS, was used to simulate and investigate deformation characteristics of different profiles. All the profiles were designed by the length of 60 mm and the maximum distortion angle of 45º. Simulation was performed using 3-D models in which the geometrical dimensions and mechanical properties of specimens in the simulation were the same for all profiles, making it possible to compare the simulation results with each other. Die and punch were assumed as rigid bodies, whereas the billets were considered to be a deformable aluminum alloy (AA1050) with the stress–strain relation of $\sigma = 106\varepsilon^{0.347}$ (MPa). The work hardening behavior was determined experimentally by compression test at room temperature. Two billets with dimension of 10mm×10mm×60 mm were simulated simultaneously (one after another).

8-node linear brick elements (C3D8R) [19] and 4-node 3-D bilinear rigid quadrilateral elements (R3D4) [19] were used to mesh the billet, and die rigid parts respectively. In addition, a 0.5 mm radius fillet was assigned to the longitudinal edges of the billet to avoid distortion of elements adjacent to this region. Number of elements for billets and die were 9900 and 3938, respectively.

The backpressure was considered in the range of 50-150 MPa. Constant friction factor at the interface between the billet and the die was determined as m=0.1 using barrel compression test [20]. In order to apply this value in simulation, it was converted to friction coefficient μ= 0.047 by using the following relation [21]:

$$\mu = \frac{m^{0.9}}{2.72(1-m)^{0.11}} . \quad (13)$$

4- Results and discussion

Fig.4 shows the final shape of the samples after SSE with different die profiles. For all die profiles, the change in the sample length (amount of waste material) is negligible, which is-the advantage of SSE process[10]. In the absence of backpressure, the die cannot completely be filled by the material .The sample shape after SSE is approximately the same for different die profiles (see Fig.4 and 5). The distribution of the equivalent strain through cross section of the samples after SSE for the proposed die profiles is shown in Fig.5. In contrast to the TE process, the largest amount of strain is determined in the center of the samples [10]. The most homogeneous distribution of strain is obtained by the linear die profile. In this case, the values of strains are somewhat larger than that of the other die profiles. The lowest value of strains and a non-homogenous distribution of strain are determined for the sinusoidal die profile. As shown in Fig.6, the type of die profile does not have a significant effect on the load of the deformation process. The maximum load required for the process is about 14500 N (1.45 tons).

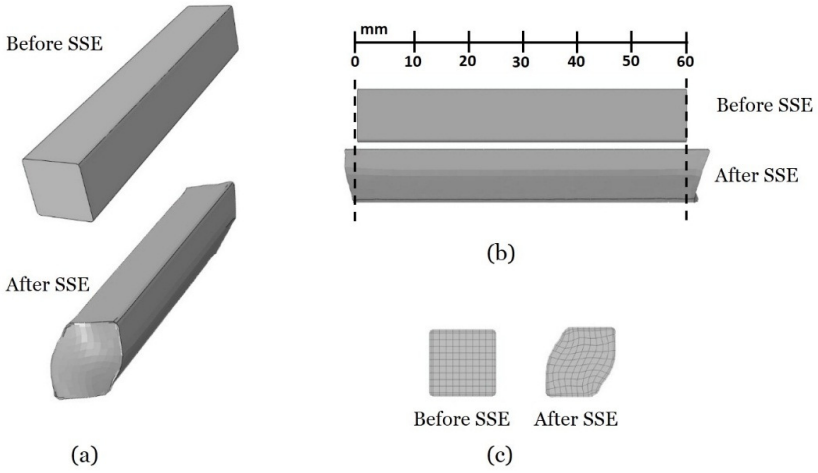

Fig.4. The sample shape before and after SSE (without back-pressure) for all die profiles, (a) 3-D view, (b) front view, (c) cross section

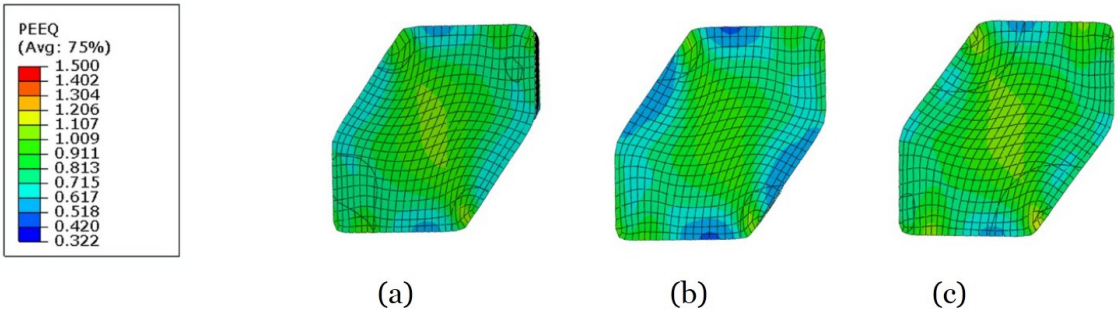

Fig.5. Distribution of equivalent strain in the cross section of samples after SSE process (without back-pressure) by (a) quadratic, (b) sinusoidal and (c) linear profiles.

The sample shape for different die profile after SSE with and without backpressure is shown in Fig.7. The least amount of back-pressure required for the quadratic, sinusoidal and linear profiles to completely fill the channel are 130 MPa, 135 MPa and 130 MPa, respectively. It is clear that by applying adequate amount of the back-pressure, the deformation channel is filled entirely and also the waste material is reduced. Results show that the quadratic and linear profiles need the same amount of back-pressure which is less than that of sinusoidal profile. Nevertheless, the minimum amount of required back-pressure for all the profiles is approximately the same. It can be concluded that the die profile cannot significantly affect the deformation load. In addition, in order to fill the channel die, approximately the same amount of backpressure is needed for all die profiles.

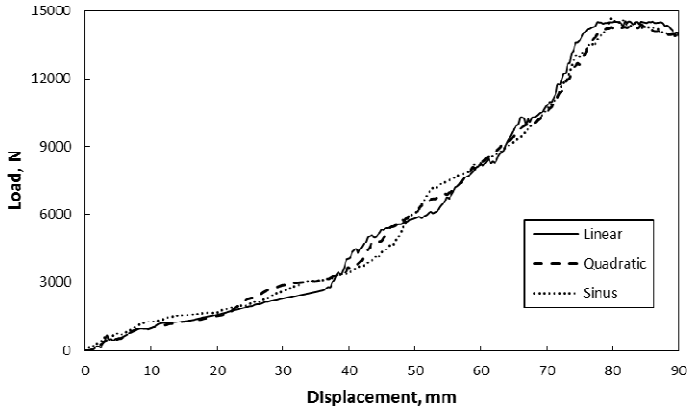

Fig.6. Comparison of processing load-displacement curves of different profiles

The theoretical shear strain through the deformation channel can be calculated by Eq. (6) for given values of the simulation variables (L=60mm, a=10mm and α_{max}=45˚). The shear strain can also determined by simulation using the finite element analysis. Fig.8 shows the variation of shear strain at the center of the samples, from the beginning to the end of the deformation channel for different profiles in the presence of the back-pressure. As can be seen, the theoretical shear strain for all the die profiles reaches to 1 at the midway of the channel where the maximum distortion angle (α_{max}) is $\pi/4$. It decreases to zero in the second half of the channel as the

specimen deforms by the same amount of shear strain in the reverse direction. The shear strains obtained by the simulations are changed in the same way.

The equivalent accumulated strain and current strain rate for all die profiles can be calculated by Eqs. (7 to 12). The values of the deformation parameters used in simulations (L=60mm, a=10mm, α_{max}=45˚and the ram speed of 0.1 mm/sec) are considered for calculation. The theoretical and simulated values of the equivalent strain and the current strain rate at the center of the sample, from the beginning to the end of the deformation channel is shown in Fig.9a and Fig. 9b, respectively. The simulated values of the strains are slightly lower than those of the theoretical values. However, the simulated and theoretical strains are changed with a similar trend in the deformation channel. For all die profiles, the strain increases gradually with increasing the distance in the deformation channel. The rate of increasing the strain for the quadratic profiles decreases at the start, middle and the end of the channel while for the sinusoidal profile it decreases only at the middle. For the linear die profile, the rate of increasing the strain remains constant through the entire channel. Fig.9b shows that the maximum strain rate of the quadratic profile is occurred at the $L/4$ and $3L/4$ distances (relative distance of 0.25 and 0.75) from the channel inlet. In the case the sinusoidal profile, the highest value of the strain rate is achieved at the entrance and the exit channel. The lowest value of strain rate for both quadratic and linear profiles is occurred at the middle of the channel (relative distance of 0.5). In accordance to Fig.4b the theoretical strain rate for the linear profile is constant through entire channel. This constant strain rate facilitates the room temperature deformation of hard to deform materials by SSE technique [16-18]. The linear die profile exhibited a deference between the theoretical and simulated strain rates at the middle of the channel. The strain rate reduces at the middle of the channel because of the strain that may postpone the straining and decrease the strain rate.

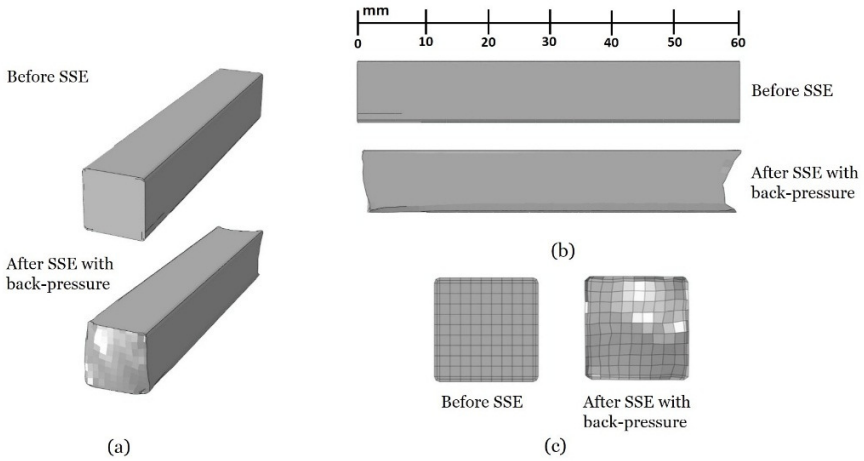

Fig.7. The sample shape before and after SSE processing (with back-pressure) for all the profiles, (a) 3-D view, (b) front view, (c) cross section

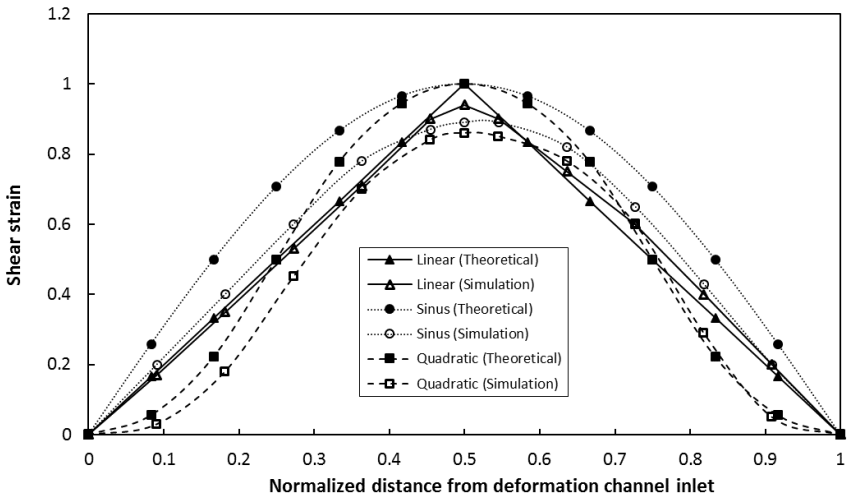

Fig.8. Variation of the shear strain at the center of sample along the extrusion channel.

The simplicity of the die design, the homogeneity of the strain and the constant strain rate, are the most important factors that make the linear die profile be a good candidate for SSE processing. More detail of deformation by the linear die profile and also the effect of the length of deformation channel on load of SSE process by this profile is the subject of authors undergoing studies.

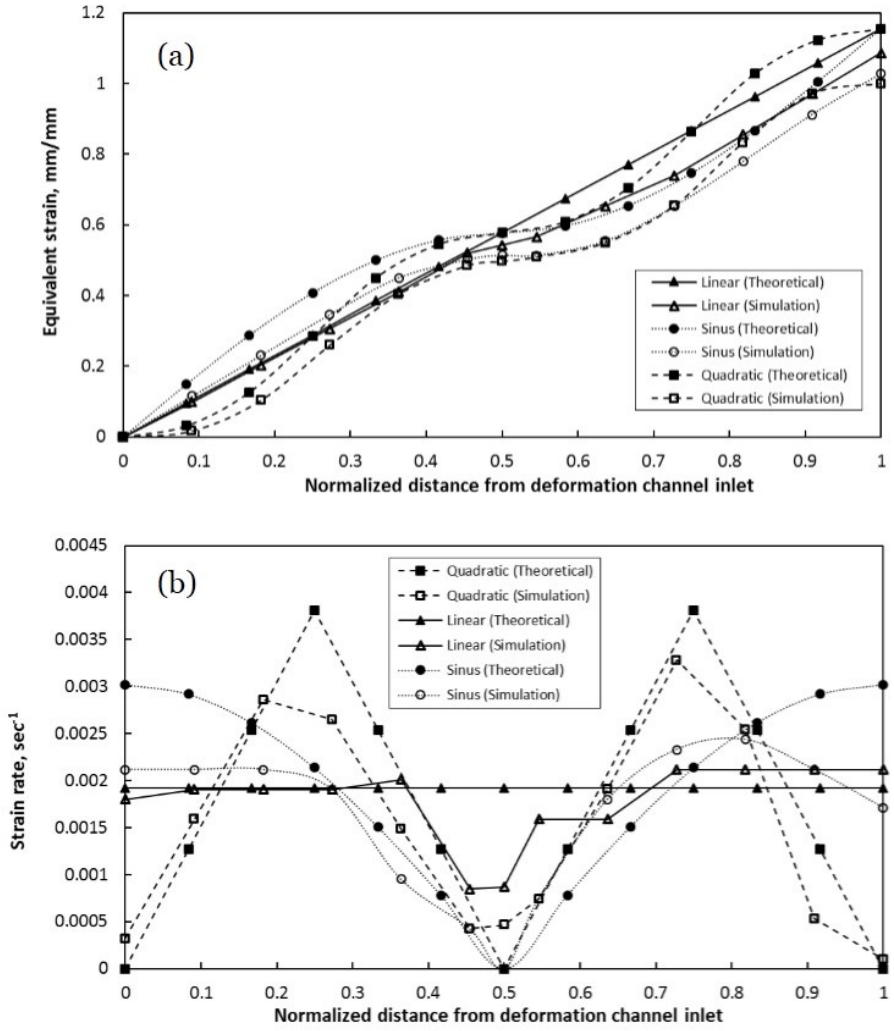

Fig.9. (a) Equivalent (or accumulated)-strain and (b) current strain rate through entire the deformation channel.

5- Conclusion

Quadratic, sinusoidal and linear profiles is introduced and the effect of these profiles on the deformation behavior during the process was investigated by finite element method using ABAQUS/Explicit package. The following results are obtained:

1- The shape of the die profile does not have a significant effect on the ~~required~~ deformation load and the required backpressure for filling the channel.
2- The most homogeneous distribution of strain is obtained in the linear die profile.
3- For all the profiles, the strain gradually increases with increasing the distance in the channel. Among all die profiles, only the linear profile can offer a constant strain rate which is a great advantage for difficult to work materials.

4- The linear die profile is the best candidate for SSE because of the simplicity of the die design, the homogeneity of the strain and its constant strain rate.

References

[1] Sabirov I, Murashkin MY, Valiev RZ, 2013, Nanostructured aluminium alloys produced by severe plastic deformation: New horizons in development, *Materials Science and Engineering: A*, **560,** 1.
[2] Valiev RZ, Islamgaliev RK, Alexandrov IV, 2000, Bulk nanostructured materials from severe plastic deformation, *Progress in Materials Science*, **45,** 103.
[3] Estrin Y, Vinogradov A, 2013, Extreme grain refinement by severe plastic deformation: A wealth of challenging science, *Acta Materialia*, **61,** 782.
[4] Valiev RZ, Langdon TG, 2006, Principles of equal-channel angular pressing as a processing tool for grain refinement, *Progress in Materials Science*, **51,** 881.
[5] Zhilyaev AP, Langdon TG, 2008, Using high-pressure torsion for metal processing: Fundamentals and applications, *Progress in Materials Science*, **53,** 893.
[6] Saito Y, Utsunomiya H, Tsuji N, Sakai T, 1999, Novel ultra-high straining process for bulk materials—development of the accumulative roll-bonding (ARB) process, *Acta materialia*, **47,** 579.
[7] Salishchev G, Zaripova R, Galeev R, Valiakhmetov O, 1995, Nanocrystalline structure formation during severe plastic deformation in metals and their deformation behaviour, *Nanostructured Materials*, **6,** 913.
[8] Beygelzimer Y, Varyukhin V, Synkov S, Orlov D, 2009, Useful properties of twist extrusion, *Materials Science and Engineering: A*, **503,** 14.
[9] Huang JY, Zhu YT, Jiang H, Lowe TC, 2001, Microstructures and dislocation configurations in nanostructured Cu processed by repetitive corrugation and straightening, *Acta Materialia*, **49,** 1497.
[10] Pardis N, Ebrahimi R, 2009, Deformation behavior in Simple Shear Extrusion (SSE) as a new severe plastic deformation technique, *Materials Science and Engineering: A*, **527,** 355.
[11] Pardis N, Talebanpour B, Ebrahimi R, Zomorodian S, 2011, Cyclic expansion-extrusion (CEE): A modified counterpart of cyclic extrusion-compression (CEC), *Materials Science and Engineering: A*, **528,** 7537.
[12] Shahbaz M, Pardis N, Ebrahimi R, Talebanpour B, 2011, A novel single pass severe plastic deformation technique: Vortex extrusion, *Materials Science and Engineering: A*, **530,** 469.
[13] Orlov D, Reshetov A, Varyukhin V, Korshunov A, Korotchenkova I, Beygelzimer Y, Vedernikova I, Polyakov L, Synkov S, Synkov A, 2006, Features of twist extrusion: method, structures & material properties, *Solid State Phenomena*, **114,** 69.
[14] Orlov D, Varyukhin V, Beygelzimer Y, Synkov S, 2006, Application of twist extrusion. Materials Science Forum, **503,** 335.
[15] Pardis N, Ebrahimi R, 2010, Different processing routes for deformation via simple shear extrusion (SSE), *Materials Science and Engineering: A*, **527,** 6153.
[16] Bagherpour E, Reihanian M, Ebrahimi R, 2012, On the capability of severe plastic deformation of twining induced plasticity (TWIP) steel, *Materials & Design*, **36,** 391.

[17] Bagherpour E, Reihanian M, Ebrahimi R, 2012, Processing twining induced plasticity steel through simple shear extrusion, *Materials & Design*, **40,** 262.
[18] Bayat Tork N, Pardis N, Ebrahimi R, 2013, Investigation on the feasibility of room temperature plastic deformation of pure magnesium by simple shear extrusion process, *Materials Science and Engineering: A*, **560,** 34.
[19] Hibbit, Karlsson, Sorensen, 2007, ABAQUS/Standard Analysis User's Manual: Hibbit, Karlsson, Sorensen Inc..
[20] Ebrahimi R, Najafizadeh A, 2004, A new method for evaluation of friction in bulk metal forming, *Journal of Materials Processing Technology*, **152,** 136.
[21] Molaei S, 2013, Study on friction in metal foming process by finite element analysis, *M.Sc. thesis*, Shiraz University.